

## LOADING RATE DEPENDENCY OF COMPLETE STRESS-STRAIN CURVE OF VARIOUS ROCK TYPES

M. Lei<sup>1</sup>, K. Hashiba<sup>2</sup>, S. Okubo<sup>3</sup> and K. Fukui<sup>4</sup>

<sup>1</sup> *Doctoral student, Dept. of Systems Innovation, The University of Tokyo, Tokyo, Japan*

<sup>2</sup> *Assistant Professor, Dept. of Systems Innovation, The University of Tokyo, Tokyo, Japan*

<sup>3</sup> *Professor, Dept. of Systems Innovation, The University of Tokyo, Tokyo, Japan*

<sup>4</sup> *Associate Professor, Dept. of Systems Innovation, The University of Tokyo, Tokyo, Japan*

*Email: leiionster@gmail.com*

### ABSTRACT:

Loading rate dependency of stress-strain curve is closely related to time-dependent behaviors such as creep, stress relaxation and viscoelasticity. But it is difficult to research the loading rate dependency of complete stress-strain curve for rock. Recently a method was proposed, in which the loading rates were alternated between slow and fast rates at a uniform strain interval. This method is so simple that special equipment or technique isn't required. With the aid of this method, two stress-strain curves corresponding to two loading rates can be estimated from just one specimen. In this study, the alternating loading rate test was applied to compression and tension tests for not only Class I rock but also Class II rock, which has a positively inclined portion of the stress-strain curve in the post-failure region. Loading rate dependency of complete stress-strain curves of Class I and Class II rocks were examined. Experimental results indicate that this testing method can be adopted to research the loading rate dependency of complete stress-strain curve of Class I and Class II rocks under various stress state.

**KEYWORDS:** rock, time-dependent behavior, loading rate, complete stress-strain curve, post-failure region

### 1. INTRODUCTION

The rheological and time-dependent behaviors of rock are the fundamental mechanical properties, which are essential in understanding the mechanism of earthquake or estimating the long-term stability of rock structures, for example tunnel, rock slope and underground storage. Ordinarily, creep, stress relaxation and loading tests are employed to investigate the time dependency of rock in laboratory (Li et al, 2000). Creep tests are relatively easy to conduct, but they need a very long time. Stress relaxation tests also require a long period of time. Loading rate dependency is closely related to other time-dependent behaviors such as creep, stress relaxation and time-dependent crack growth (Lajtai et al, 1986), and so it has been investigated by many researchers.

Loading test is generally conducted at constant loading rate. Due to the inhomogeneity of rock, many samples are required in the loading tests at different loading rates. It costs a lot of time and effort to investigate the loading rate dependency of rock with the ordinary testing method. So a testing method, in which a single rock specimen was loaded at alternating loading rate, was proposed to obtain the properties concerning the time dependency of rock and applied to uniaxial and triaxial compression tests (Hashiba et al, 2006). But until now little knowledge concerning the loading rate dependency of complete stress-strain curve has been obtained in compression. Much time and technical skills are required in uniaxial tension test. So, not enough researches have been done to investigate the loading rate dependency of complete stress-strain curve in tension. Failures under tensile stress are the basic mechanism of rock and become more and more serious in the large underground structures (Fukui et al, 2003; Lankford, 1981; Okubo et al, 2006). And especially for Class II rocks, there still remain a lot of things unknown about the loading rate dependency of complete stress-strain curve or in the post-failure region.

In this paper, the proposed alternating loading rate testing method was applied to uniaxial compression, uniaxial tension and indirect tension (Brazilian) tests with not only Class I but also Class II rocks. Loading rate dependency of complete stress-strain curve, peak strength and residual strength were examined with this method. The loading rate dependency of complete stress-strain curves was compared between two rock types and various loading conditions. The experimental data in this study was compared with those obtained from ordinary testing methods in previous studies. And the loading rate dependency was compared between peak and residual strengths. It is possible to derive the values of constants in viscoelastic constitutive equations of rock from the experimental data obtained in this study. And it helps us to estimate the long-term stability of rock structures or to understand the mechanism of earthquake.

## 2. ROCK SAMPLES AND TESTING METHOD

Rock samples are Sanjome andesite and Tage tuff obtained in Japan. Sanjome andesite was employed in uniaxial compression, uniaxial tension and indirect tension tests. Tage tuff was employed in indirect tension test. Previous data of Tage tuff in uniaxial compression and uniaxial tension tests (Hashiba et al, 2006; Fukui et al, 2003) were reexamined. The specimens were 25 mm in diameter and 50 mm in length for the uniaxial compression and uniaxial tension tests, and 25 mm in diameter and 12.5 mm in thickness for the indirect tension test. All of the specimens were air dried in the laboratory for at least two weeks before testing.

A digital servo-controlled testing machine with a capacity of 500 kN was employed in uniaxial compression and tension tests. Indirect tension tests were performed with a 10 kN servo-controlled testing machine. The load was measured with a strain-gauge type load cell, and the displacement was measured with an LVDT. A linear combination of displacement and load,  $U - \alpha F / E$ , was used as a control variable in the servo-controlled testing machine (Okubo et al, 1985). Here,  $U$  is displacement,  $F$  is load,  $E$  is the Young's modulus of rock, and  $\alpha$  is a constant. In the method, the loading rate  $\dot{U} - \alpha \dot{F} / E$  was alternated between a slow rate  $C_1$  and a fast one  $C_2$  at a constant strain interval in uniaxial compression and tension tests or at a constant displacement interval in indirect tension test. Load increased abruptly when the loading rate was increased, and decreased abruptly when the loading rate was decreased (Hashiba et al, 2006). The testing conditions are shown in Table 2.1 and Table 2.2.

Table 2.1 Rock samples and testing conditions in compression (UCT) and tension (UTT) tests

Rock type	Loading rate ( $\times 10^{-6}/s$ )		Strain interval ( $\times 10^{-6}$ )	
	UCT	UTT	UCT	UTT
Tage tuff	10↔100	1↔10	300, 500	100
Sanjome andesite	10↔100	1↔10	300, 500	50

Table 2.2 Rock samples and testing conditions in indirect tension test (ITT)

Rock type	Loading rate ( $\times 10^{-4}$ mm/s)	Displacement interval ( $\times 10^{-3}$ mm)
Tage tuff	1↔10, 0.5↔5, 0.5↔10	5, 8
Sanjome andesite	1↔10, 0.5↔5, 0.5↔10	5, 10

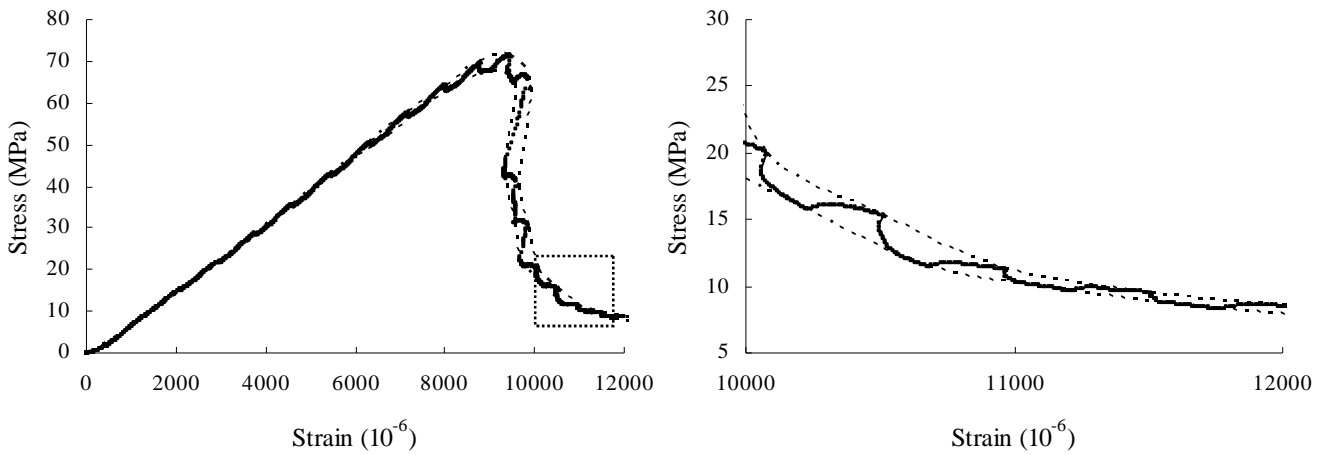
## 3. EXPERIMENTAL RESULTS

### 3.1. Uniaxial Compression Test

In Figure 1 and 2, thick lines show the stress-strain curves of Sanjome andesite and Tage tuff obtained from the alternating loading rate compression tests. For Sanjome andesite in Figure 1, there is little variation in stress with the changes of loading rate at the beginning of experiment. Then above the stress level about 50% of peak strength, stress fluctuates with the change of loading rate. Stress fluctuation can be clearly seen near the peak strength. For Sanjome andesite, stress decreases almost vertically after peak strength, but loading rate was alternated under control. The stress-strain curve framed by dotted line is magnified as shown in Figure 1(b).

Stress fluctuation can be still observed until the stress level about 10% of peak strength. Loading rate dependency of residual strength can be clearly observed in the post-failure region.

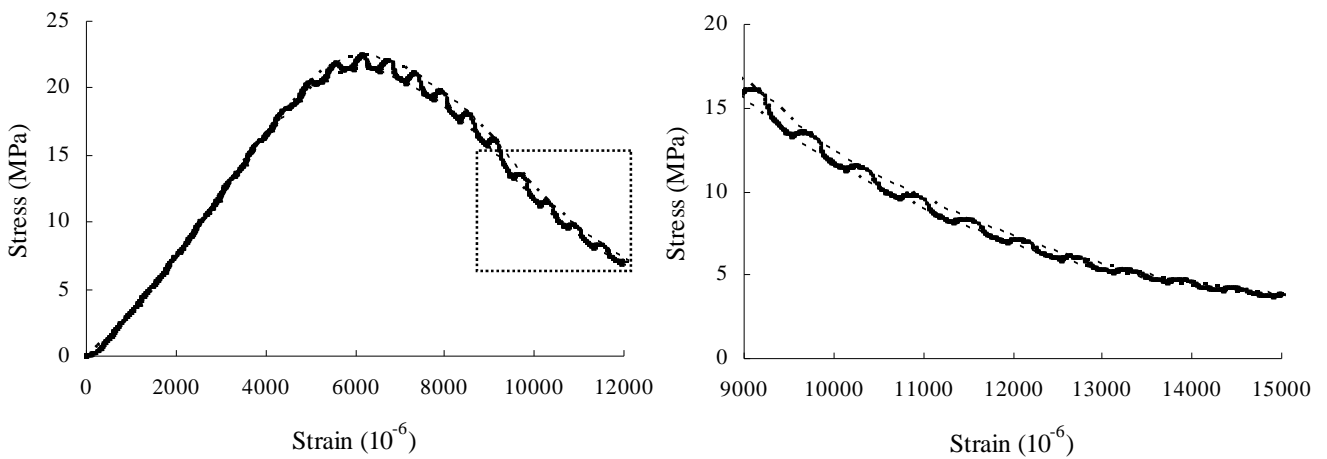
As for Tage tuff in Figure 2 (Hashiba et al, 2006), below the stress level about 50% of peak strength in the pre-failure region, stress fluctuation is not obvious. With the increase of stress, stress fluctuation can be clearly seen. After peak strength, stress decrease with the increase of strain. The stress-strain curve framed by dotted line is magnified as shown in Figure 2(b). For the complete stress-strain curve, loading rate dependency can be clearly observed.



(a) Complete stress-strain curve

(b) Magnified part in the post-failure region

Figure 1 Stress-strain curve for Sanjome andesite in uniaxial compression test



(a) Complete stress-strain curve

(b) Magnified part in the post-failure region

Figure 2 Stress-strain curves for Tage tuff in uniaxial compression test (Hashiba et al, 2006)

### 3.2. Uniaxial Tension Test

The stress-strain curves of Sanjome andesite and Tage tuff in uniaxial tension tests are shown in Figure 3 and 4 with thick lines. For Sanjome andesite in Figure 3, below the stress level about 70% of peak strength, stress fluctuation with the change of loading rates is not obvious. As the stress increase further, stress fluctuations

become bigger and can be clearly observed. After peak strength, there is an abrupt decrease of stress. Stable alternation of loading rate can be carried out under control. The stress-strain curve framed by dotted line is magnified as shown in Figure 3(b). In the post-failure region, even under a very small stress level, stress fluctuation can be clearly observed.

As for Tage tuff in Figure 4 (Fukui et al, 2003), the same as Sanjome andesite, under small stress level before peak strength, stress fluctuation is not obvious. Stress fluctuation become bigger as the increase of stress. Near peak strength, loading rate dependency of peak strength can be clearly observed. After peak strength, stress decreases with the increase of strain. The stress-strain curve framed by dotted line is magnified as shown in Figure 4(b). In the post-failure region, stress fluctuation can be observed even under small stress level.

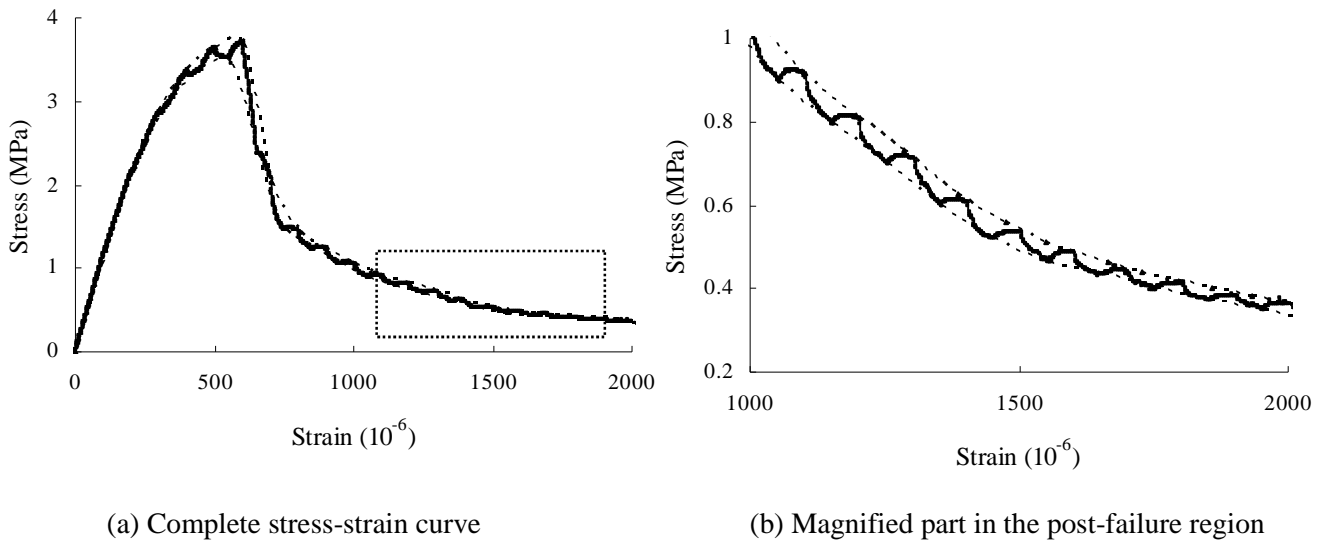


Figure 3 Stress-strain curves for Sanjome andesite in uniaxial tension test

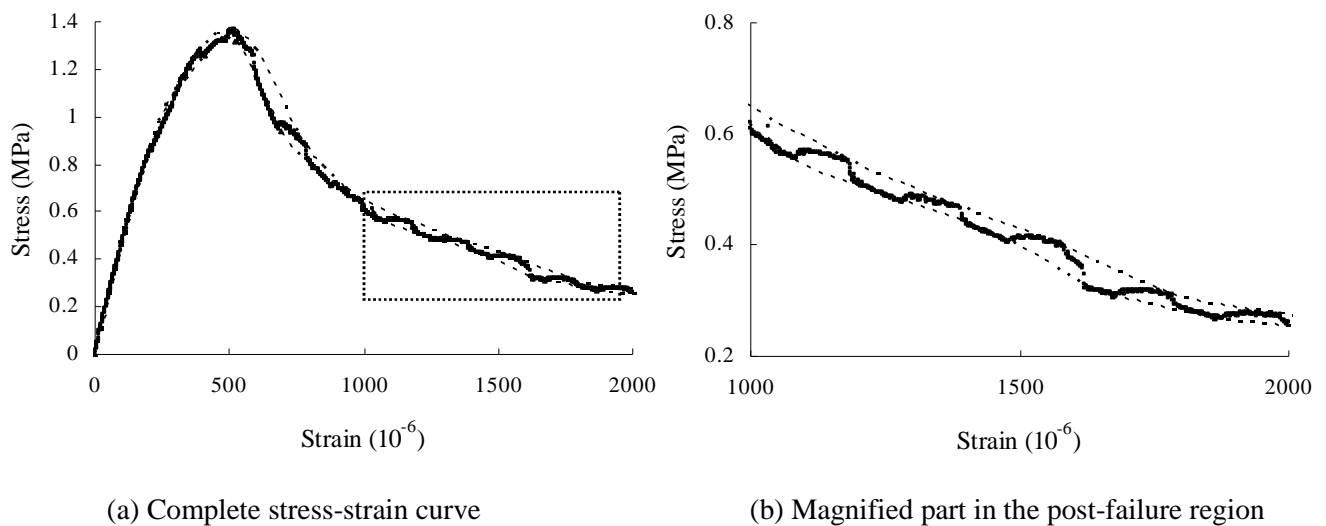


Figure 4 Stress-strain curves for Tage tuff in uniaxial tension test (Fukui et al, 2003)

### 3.3. Indirect tension test

As for Sanjome andesite in Figure 5, the fluctuation of load is not distinct in the pre-failure region, and there is

an abrupt failure just after peak load. The load-displacement curve framed by dotted line is magnified as shown in Figure 5(b). In the post-failure region some parts of the specimen peel off or spall gradually, so a few peaks are observed in this region.

As for Tage tuff in Figure 6, the fluctuation of load with loading rate is not distinct until the stress level about 40% of peak load. Above this load level, fluctuation of load can be also observed clearly. After the peak load, load decreases slowly with the central crack crossing through the specimen. Then the load-displacement curve becomes almost flat. The load-displacement curve framed by dotted line is magnified as shown in Figure 6(b). Likewise, the fluctuation of load can be still observed in this region.

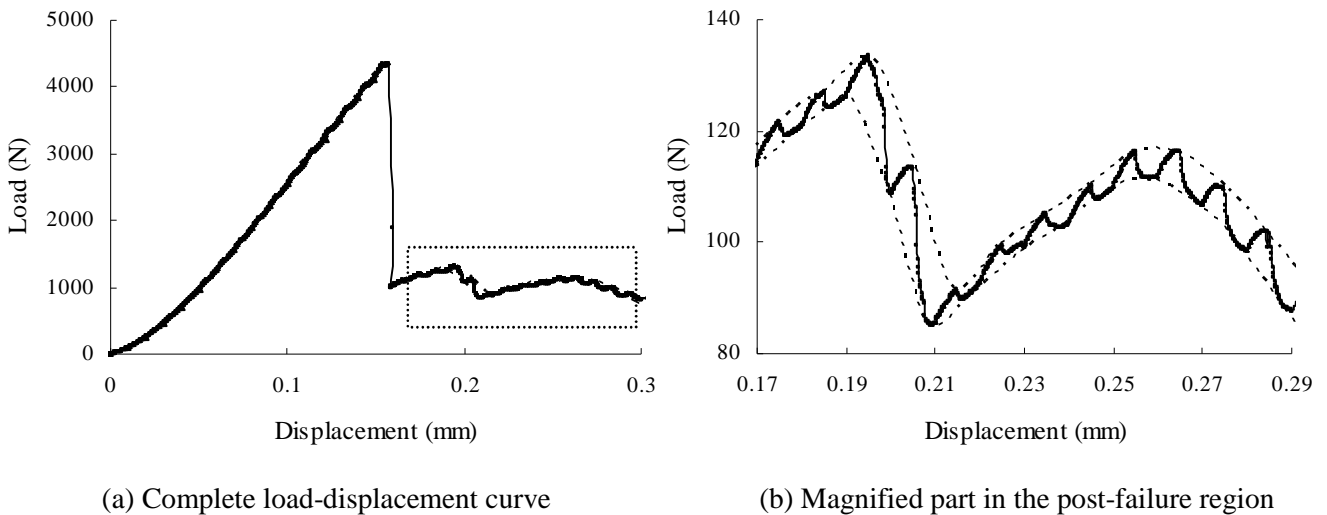


Figure 5 Load-displacement curves for Sanjome andesite in indirect tension test

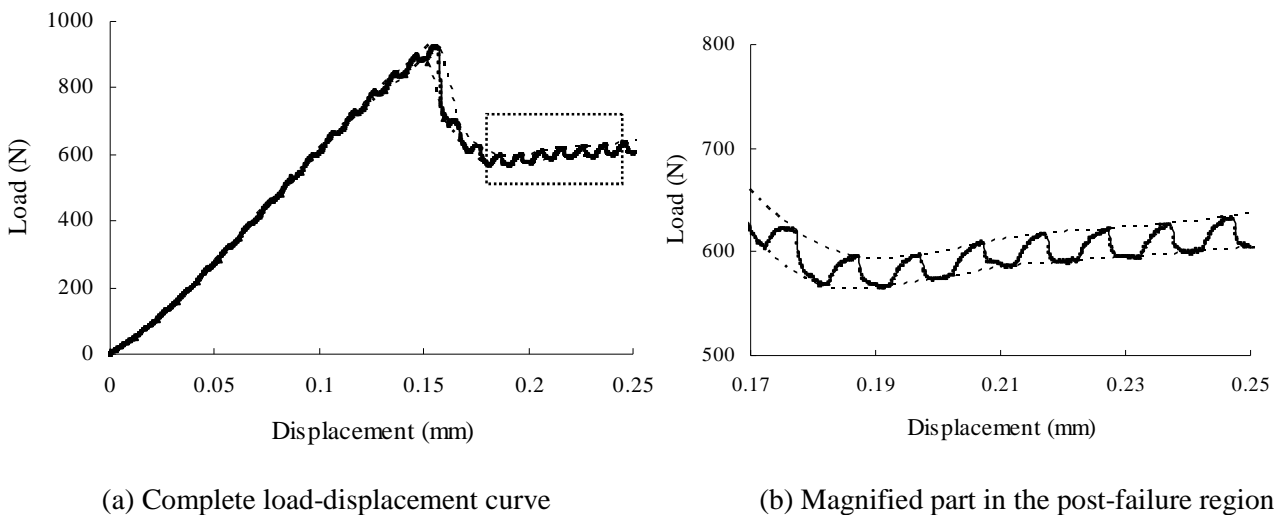


Figure 6 Load-displacement curves for Tage tuff in indirect tension test

From the above experimental data, it is found that alternating loading rate tests can be applied to compression and tension tests. Stress-strain curves are different due to different kinds of rock. As for Class I rock, after peak strength, stress decreases slowly and gently with the increase of axial strain in compression and tension tests. As for Class II rock, there was an abrupt decrease of stress immediately following the peak strength. But loading rate still can be alternated under control in the post-failure region in both compression and tension tests. Loading rate dependency was clearly observed not only at peak strength but also in the post-failure region. From the

viewpoint of experimental phenomena of compression and tension tests, just before the peak strength, outside part of the test specimen began to peel off and a big diagonal crack crossed it in compression, while there was only a small crack crossing the specimen in tension. In the post-failure region, outside part of the specimen continued to peel off and dropped, specimen almost turned into double cone shape in compression. While in the post-failure for tension test obvious changes can not be observed.

For indirect tension test, an obvious crack crossing the center of the specimen can be seen, and then stress began to decrease just after the peak load. The alternating loading rate indirect tension test is easier to conduct and requires smaller amount of rock samples than uniaxial tension test. So it will be a useful testing method to investigate the loading rate dependency in tension, but now it is difficult to control just after peak load with brittle rock and to specify the stress state in the post-failure region.

#### 4. LOADING RATE DEPENDENCY OF PEAK AND RESIDUAL STRENGTH

Many rocks are known to exhibit a small increase of peak strength over orders of magnitude of increasing loading rate (Sano et al, 1981; Swan et al, 1989). The fluctuations of stress or load with the change of loading rate in the alternating loading rate tests have a close relation with the loading rate dependency of stress-strain or load-displacement curve. So, as shown in Figure 1 to 6, the lower dashed line was drawn by connecting the points just before loading rate increased, and considered as the stress-strain or load-displacement curve for the slow loading rate  $C_1$ . In the same way, the upper dashed line was drawn by connecting the points just before loading rate decreased, and considered as the stress-strain or load-displacement curve for the fast loading rate  $C_2$ . The schematic graph is shown in Figure 7.

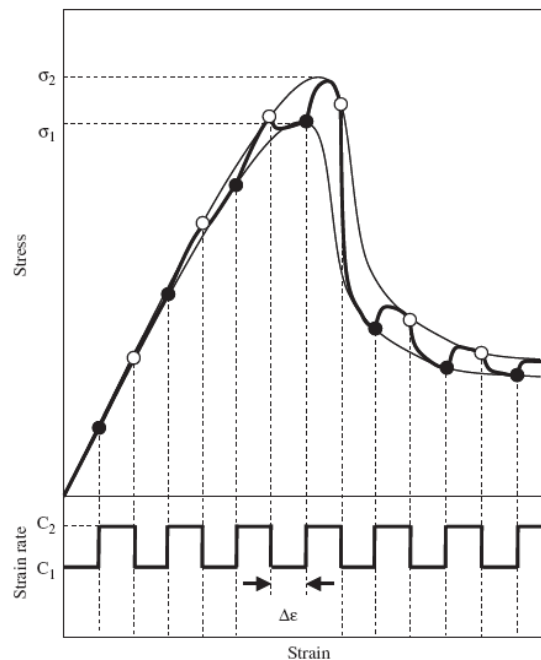


Figure 7 Schematic graph of stress-strain curve in alternating strain rate test (Hashiba et al, 2006)

In the previous studies, many rocks show an increase of peak strength with loading rate as follows (Lankford, 1981; Lei et al, 2008):

$$\sigma_2 / \sigma_1 = (C_2 / C_1)^{1/n+1} \quad (4.1)$$

where,  $\sigma_1$  and  $\sigma_2$  are the peak strengths corresponding to the loading rate  $C_1$  and  $C_2$ , respectively.  $n$  is the parameter of loading rate dependency.

According to Eqn.4.1, loading rate dependency of peak strength was investigated. The results are listed in Table 4.1. Values of parameter  $n$  at peak strength in compression were a little larger than those in tension, but due to the scatter of data, they are almost the same under compressive and tensile stress state. And values obtained in this study are consistent with those obtained from ordinary constant loading rate tests in uniaxial compression, uniaxial tension and indirect tension tests (Okubo et al, 2006). So the alternating loading rate testing method can be adopted to investigate the loading rate dependency of peak strength in compression and tension tests with not only Class I but also Class II rocks.

Table 4.1 Average values of parameter  $n$  at peak strength in the different testing conditions

Rock type	Testing conditions					
	UCT		UTT		ITT	
	A.V	C.V (%)	A.V	C.V (%)	A.V	C.V (%)
Tage tuff	51	3.6	46	7.2	43	10.3
Sanjome andesite	41	2.1	37	11.3	-	-

A.V: average value, C.V: coefficient of variation

Little knowledge concerning the loading rate dependency in the post-failure region has been obtained in previous studies. So, Eqn.4.1 was extended to the post-failure region to investigate the loading rate dependency of residual strength (Hashiba et al, 2005). In the post-failure region, there have not been specific methods for calculating parameter  $n$ . In order to calculate parameter  $n$ , three kinds of proposed methods as shown in Figure 8 were applied (Fukui et al, 2003).

1. Using the stresses  $\sigma_1$  and  $\sigma_2$  corresponding to  $C_1$  and  $C_2$  at the same strain.
2. Using the stresses  $\sigma_1$  and  $\sigma_2$  at the intersections of the straight line crossing the original point with the two stress-strain curves corresponding to  $C_1$  and  $C_2$ .
3. Using the stresses  $\sigma_1$  and  $\sigma_2$  at the intersections of the tangential lines of unloading curves with the two stress-strain curves corresponding to  $C_1$  and  $C_2$ .

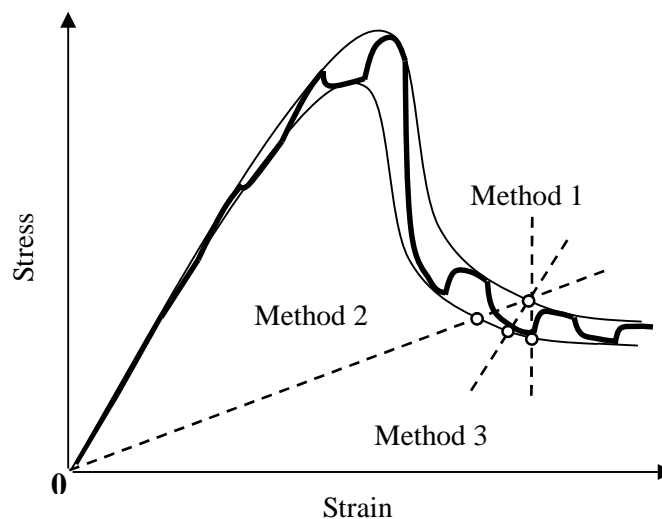


Figure 8 Schematic graph of computing parameter  $n$  in the post-failure region

In this paper, using method 1 and method 2, values of parameter  $n$  of residual strength were calculated, and listed in Table 4.2. In contrast to the values of parameter  $n$  of peak strength, values of residual strength in uniaxial compression tests were larger than those in uniaxial tension tests with both methods. But the values of parameter  $n$  at peak strength are between those of residual strength obtained from method 1 and method 2 in

Table 4.2 Values of parameter  $n$  in the post-failure region with the two proposed methods

Rock type	Method 1				Method 2			
	UCT		UTT		UCT		UTT	
	A.V	C.V (%)	A.V	C.V (%)	A.V	C.V (%)	A.V	C.V (%)
Tage tuff	37	18.5	25	27.1	115	9.1	66	23.4
Sanjome andesite	25	24.5	18	29.6	108	9.1	54	18.1

A.V: average value, C.V: coefficient of variation

compression and tension. The stress-strain curves of rock in post-failure region have large scatter from specimen to specimen, so the alternating loading rate testing method will be a useful tool to investigate the loading rate dependency in post-failure region or residual strength in various testing conditions with not only Class I but also Class II rocks.

## 5. CONCLUSION

Loading rate dependency is an essential factor of the viscoelasticity of rock. In this paper, the alternating loading rate tests under compressive and tensile stress states were conducted. Loading rate dependency of complete stress-strain curve can be investigated even under a small stress level in the post-failure region. The values of parameter  $n$  at peak strength can well coincide with those obtained from ordinary methods. Values of parameter  $n$  were also calculated in the post-failure region. This proposed testing method is feasible to investigate the loading rate dependency of complete stress-strain curves of rock from a small number of samples.

## REFERENCES

- Fukui, K., Okubo, S. and Iwano, K. (2003). Loading rate dependency of Sanjome andesite and Tage tuff in uniaxial tension. *Journal of JSCE*, **729:III-62**, 59-71. (in Japanese)
- Hashiba, K., Okubo, S. and Fukui, K. (2005). Loading rate dependency of peak and residual strengths of rocks. *Journal of MMIJ*, **121:1**, 11-18. (in Japanese)
- Hashiba, K., Okubo, S. and Fukui, K. (2006). A new testing method for investigating the loading rate dependency of peak and residual rock strength. *Int. J. Rock Mech. & Min. Sci.*, **43:6**, 894-904.
- Lankford, J. (1981). The role of tensile microfracture in the strain rate dependence of compressive strength of fine-grained limestone—Analogy with strong ceramics. *Int. J. Rock Mech. & Min. Sci.*, **18**, 173-175.
- Lajtai, E. Z., Bielus, L. P. (1986). Stress corrosion cracking of Lac du Bonnet granite in tension and compression. *Rock Mechanics and Rock Engineering*, **19:2**, 71-87.
- Li, Y. S. and Xia, C. C. (2000). Time-dependent tests on intact rocks in uniaxial compression. *Int. J. Rock Mech. & Min. Sci.*, **37:3**, 467-475.
- Lei, M., Hashiba, K., Okubo, S. and Fukui, K. (2008). Loading rate dependency of rock in the post-failure region under compression and tension, *Proc. of the spring meeting of MMIJ (I)*, 65-66.
- Okubo, S., Nishimatsu, Y. (1985). Uniaxial compression testing using a linear combination of stress and strain as the control variable. *Int. J. Rock Mech. Min. Sci. & Geomech. Abstr.* **22:5**, 323-330.
- Okubo, S., Fukui, K and Qi, Q. X. (2006). Uniaxial compression and tension tests of anthracite and loading rate dependence of peak strength. *Int. J. Coal Geol.*, **68:3-4**, 196-204.
- Sano, O., Ito, I., Terada, M. (1981). Influence of strain rate on dilatancy and strength of Oshima granite under uniaxial compression. *J. of Geophys. Res.*, **86:B10**, 9299-9231.
- Swan, G., Cook, J., Bruce, S. and Meehan, R. (1989). Strain rate effects in Kimmeridge Bay Shale. *Int. J. Rock Mech. Min. Sci. & Geomech. Abstr.* **26:2**, 135-149.